Chapter 3

Numerical Simulation of Flows past Bluff Bodies

Flows past bluff bodies involve complex phenomena such as separation and reattachment, unsteady vortex shedding, high turbulence, large-scale turbulence structures as well as curved shear layers. In addition, these phenomena are greatly affected by the mean-flow and turbulence characteristics of the incident flow. In many applications, there is a need to predict flow characteristics around bluff bodies and associated pressure and friction loading on these bodies. In this chapter, we review the different simulation techniques with the purpose of showing the requirements and expected results from these techniques. In addition, we explain which flow components or characteristics are considered by surface-vorticity modeling.

3.1 Governing equations

In treating the problem of fluidflow around a surface-mounted prism, one can take advantage of the two basic approaches used to describe fluid flows. The most commonly used approach is the Eulerian approach whereby one examines flow properties such as pressure and velocity as functions of space and time. Based on this approach, the flow field is governed by the Navier-Stokes equations written as

$$\frac{\partial u_j}{\partial x_j} = 0 \qquad (3.1.1)$$

$$\frac{\partial u_i}{\partial t} + \frac{\partial}{\partial x_j} u_i u_j = -\frac{1}{\rho}\frac{\partial p}{\partial x_i} + \nu \nabla^2 u_i \qquad (3.1.2)$$

where u_i represents the velocity field, p denotes the pressure, ρ is the fluid density and ν is the kinematic viscosity. In considering the flow around a surface-mounted prism, the major feature to be dealt with is that the velocity at every point in the flow varies irregularly; a feature referred to as turbulence. In the following section, we describe some of the different approaches used to solve the Navier-Stokes equations for flowfields such as those over a surface-mounted prism. In section 3.3, we describe the vorticity modeling and explain the major differences among the simulations of turbulent flows presented in section 3.2.

3.2 Simulation of turbulent flow fields

It is important to realize that turbulence is always three-dimensional, unsteady, rotational and most importantly irregular. Yet, and because the continuum assumption is valid for turbulent flows, the Navier-Stokes equations are valid. Consequently, one way to predict or simulate turbulent flows is by solving directly the instantaneous Navier-Stokes equations; an approach referred to as Direct Numerical Simulation (DNS). To perform DNS, the flow region is usually discretized by a suitable grid. The grid size is of course of utmost importance since it must be smaller than the finest turbulence scale that needs to be captured. By the finest scale, it is meant the scale responsible for the viscous dissipation of turbulent kinetic energy. Of course, the size of the finest scale depends on the Reynolds number, Re. As Re increases, the range of scales increases, and consequently, the required number of grid points increases. Because the ratio of the largest to the smallest length scale is proportional to $Re^{3/4}$ [8], one should expect that the number of grid points required by DNS to be proportional to $Re^{9/4}$. Thus for a flow with Re of about 10^7, such as encountered in wind engineering applications, the number of points would be higher than 10^{10}. This is based on a constant of proportionality obtained from similarly complex flow. Moreover, the time advancement in a DNS must resolve the time scale of the smallest

eddies. For homogeneous isotropic turbulence, the CPU time is of the order of Re^3. For other flows, the CPU time scales with the number of grid points raised to the power of 4/3 (Ragab, 1996). Thus, it is obvious that a DNS for a flow around a surface-mounted prism at a Re of 10^7 would require large computer memory and high processing speed.

Another approach to solve Navier-Stokes equations is Large Eddy Simulation (LES). In LES, a model is used to simulate the effects of the fine scales. The three-dimensional, time-dependent large-eddy structures of the turbulent flows are then calculated. The basis for this separation is the assumption of homogeneity and universality of small-scale structures. To separate the large from the small scales, LES uses a filtering operation defined by

$$\bar{u}(\mathbf{x},t) = \int_D u(\mathbf{x}',t)G(\mathbf{x},\mathbf{x}')d\mathbf{x}' \qquad (3.2.1)$$

where D is the entire domain and G is the filter function, which determines the size and structure of the small scales. Applying the filtering operation (3.2.1) to the governing equations, one obtains the filtered Navier-Stokes equations, which are solved in LES. For an imcompressible flow of a Newtonian fluid, they take the following form:

$$\frac{\partial \bar{u}_i}{\partial x_i} = 0 \qquad (3.2.2)$$

$$\frac{\partial \bar{u}_i}{\partial t} + \frac{\partial}{\partial x_j}(\bar{u}_i \bar{u}_j) = -\frac{1}{\rho}\frac{\partial \bar{p}}{\partial x_i} - \frac{\partial \tau_{ij}}{\partial x_j} + \nu \frac{\partial^2 \bar{u}_i}{\partial x_j \partial x_j} \qquad (3.2.3)$$

The effect of the small scales appears through a subgrid-scale (SGS) stress term,

$$\tau_{ij} = \overline{u_i u_j} - \bar{u}_i \bar{u}_j \qquad (3.2.4)$$

To close the system, the SGS stress terms are be modeled. One model is the Smagorinsky model (Smagorinsky, 1963) which relates the SGS to the rate-of-strain tensor by a coefficient which is constant over the whole domain of the solution and does not vary with time. Another model was given by Germano et al. (1991) and allows for the coefficient to be a function of space and time, and is referred to as the dynamic model.

The resolution required by LES is nearly independent of the Reynolds number for flows without solid surfaces. Thus LES can give significant improvement over DNS, and can be

extended to flows at Reynolds numbers at least one order of magnitude higher than DNS at a reasonable cost. On the other hand, in those cases where a solid surface is present, the simulation remains expensive unless approximate boundary conditions, or wall models, are used. In general, LES is similar to DNS in that it provides a three-dimensional, time dependent solution of the Navier-Stokes equations. Thus, it still requires fairly fine meshes.

In many applications, the interest is in the mean effect of turbulence more than in the instantaneous flow characteristics. Under these conditions, the approach is to model the average turbulence quantities. By Applying time- or ensemble-averaged operator to the Navier-Stokes equations (3.1.1-3.1.2), one obtains the Reynolds-Averaged Navier-Stokes equations (RANS):

$$\frac{\partial \langle u \rangle_i}{\partial x_i} = 0 \qquad (3.2.5)$$

$$\frac{\partial \langle u \rangle_i}{\partial t} + \frac{\partial}{\partial x_k}(\langle u \rangle_k \langle u \rangle_i) = -\frac{1}{\rho}\frac{\partial \langle p \rangle}{\partial x_i} + \frac{\partial}{\partial x_k}(\nu \frac{\partial \langle u_i \rangle}{\partial x_k} - \tau_{ik}) \qquad (3.2.6)$$

where $\tau_{ik} = \langle u_i u_k \rangle - \langle u_i \rangle \langle u_k \rangle$ are the Reynolds stresses which are usually modeled. A very wide range of models for Reynolds stresses is available, ranging from simple, algebraic models to differential linear and nonlinear forms that relate turbulent kinetic energy *k* to energy dissipation ε.

The RANS approach suffers from one principal shortcoming: the fact that the model must represent a very wide range of scales [5]. While the small scales tend to depend only on viscosity, and may be somewhat universal, the large ones are affected very strongly by the boundary conditions. Thus, it does not seem possible to model the effect of the large scales of turbulence in the same way in flows that are very different. Some adjustment of the constants is often required, which in turn implies that experimental data must be available for the flow under consideration.

3.3 Vorticity modeling

In this section, we present the background for flow modeling with vorticity. The concepts which form the basis for such modeling are explained. The governing equations and their characteristics are detailed. The application to two-dimensional flows and transformations needed to reduce the calculations are discussed. Differences from simulation of turbulent flows as summarized in section 3.2 are pointed out.

3.3.1 Basic ideas of surface vorticity modeling

The surface vorticity method, used to model potential flows and originally contrived for hand calculations, uses vortex distributions to model boundary layers and free vortex sheets. This is a quite natural approach consistent with the well known properties of vortex singularities. It has been shown that the potential flow past a body placed in a uniform stream can be modeled by replacing the body surface with a vortex sheet. In a surface vorticity model, the body surface is divided into panels and each of these panels is given a vorticity density γ_n. Each panel induces a velocity $d\vec{V}_{mn}$ at another panel located at $\vec{r}_{mn}$ as shown in Fig. 3.1. Integral equations can then be written expressing the Neumann boundary condition of zero normal surface velocity or the Dirichlet condition of zero parallel surface velocity [3].

Surface vorticity modeling results in a direct simulation of an ideal fluid flow. In all real flows a boundary viscous shear layer exists adjacent to the body surface. Invisicid potential flow is thus the limiting case of the flow of a real fluid for which the boundary layer is of infinitesimal thickness. This can be considered as the case of an infinite Reynolds number. Under this assumption, the boundary layer vorticity is squeezed into an infinitely thin vorticity sheet (basically of zero thickness) across which the velocity parallel to the surface changes discontinuously from zero in contact with the wall to the potential flow value just outside the vorticity sheet.

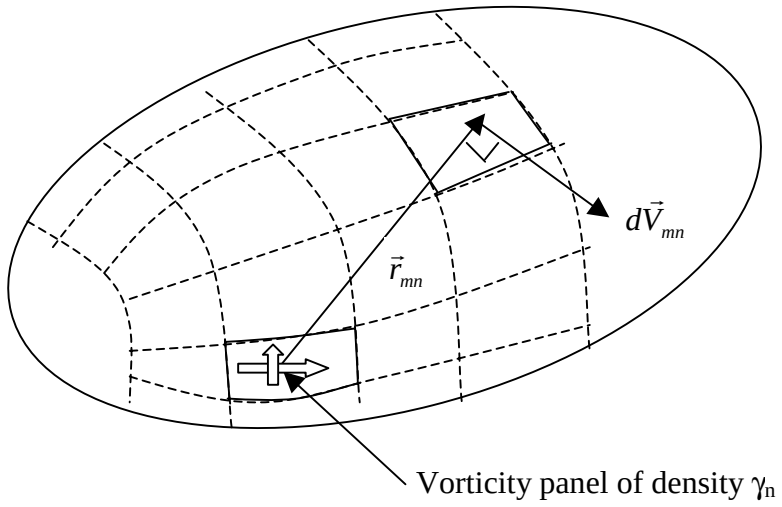

Fig. 3.1 Surface vorticity model

3.3.2 Governing equations for vortex dynamics

For incompressible flows, the continuity equation is written as

$$\nabla \bullet \vec{V} = 0 \qquad (3.3.2.1)$$

Where $\vec{V}$ is the velocity vector.

The vorticity $\vec{\Omega}$ is defined

$$\vec{\Omega} = \nabla \times \vec{V} \qquad (3.3.2.2)$$

When the flow is incompressible, Equation (3.3.2.2) can be inverted to give $\vec{V}$ as a fuction of $\vec{\Omega}$

$$\vec{V}(\vec{r},t) = \frac{1}{4\pi}\int_{Vol} \frac{\vec{\Omega}(\vec{r}_0,t)\times(\vec{r}-\vec{r}_0)}{\left|\vec{r}-\vec{r}_0\right|^3} dVol + \vec{V}_\infty \qquad (3.3.2.3)$$

Equation (3.3.2.3) shows how the velocity associated with a known vorticity can be calculated and is known as the Biot-Savart law. *Vol* is the entire region of interest (the entire vorticity-containing region), $\vec{r}_0$ is the position of the volume element d*Vol*, $\vec{r}$ is the position where the velocity is being evaluated, *t* is the time, and $\vec{V}_\infty$ is the freestream velocity. Fig. 3.2 illustrates equation (3.3.2.3).

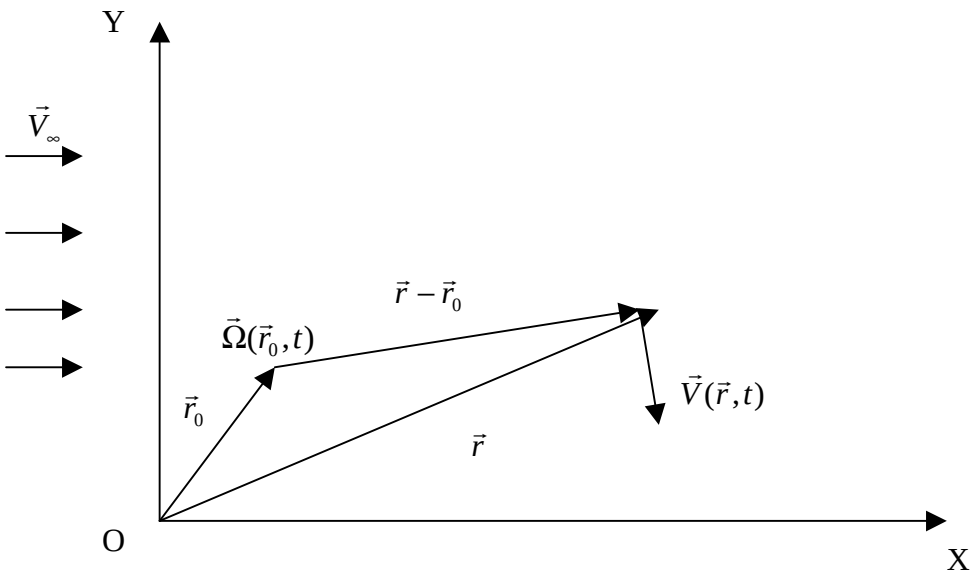

Fig. 3.2 Velocity induced by vorticity

There are several important characteristics of the velocity field $\vec{V}$ which are worth mentioning. First, the region V includes the flowfield as well as the interiors of the bodies in the flowfield. Second, it should be noted that $\vec{\Omega}$ may be zero in large subregions of V and consequently, the flowfield is irrotational in these regions. Third, the vorticity anywhere in V

induces velocity everywhere in V. Fourth, the velocity given by Equation (3.3.2.3) decays as the reciprocal of the distance from the vorticity-bearing subregions. Finally, Equation (3.3.2.3) is a purely kinematic relationship, i.e. one does not need to make any assumptions regarding the velocity field other than that $\vec{V}$ is single-valued and $\nabla \bullet \vec{V} = 0$. Consequently, Equation (3.3.2.3) is valid for "viscous" as well as "inviscid" flows.

3.3.3 Surface vorticity model for plane two-dimensional flow

Consider the flow past a two-dimensional body in the (x, y) plane, immersed in a uniform stream $\vec{V}_\infty$ as shown in Fig. 3.3. Applying the vorticity-surface method, we represent the surface of the prism by a distributed vorticity sheet initially of unknown strength. This sheet is of infinitesimal thickness and is defined at any point by the circulation per unit length γ, which is equal to the local velocity of the fluid next to the surface.

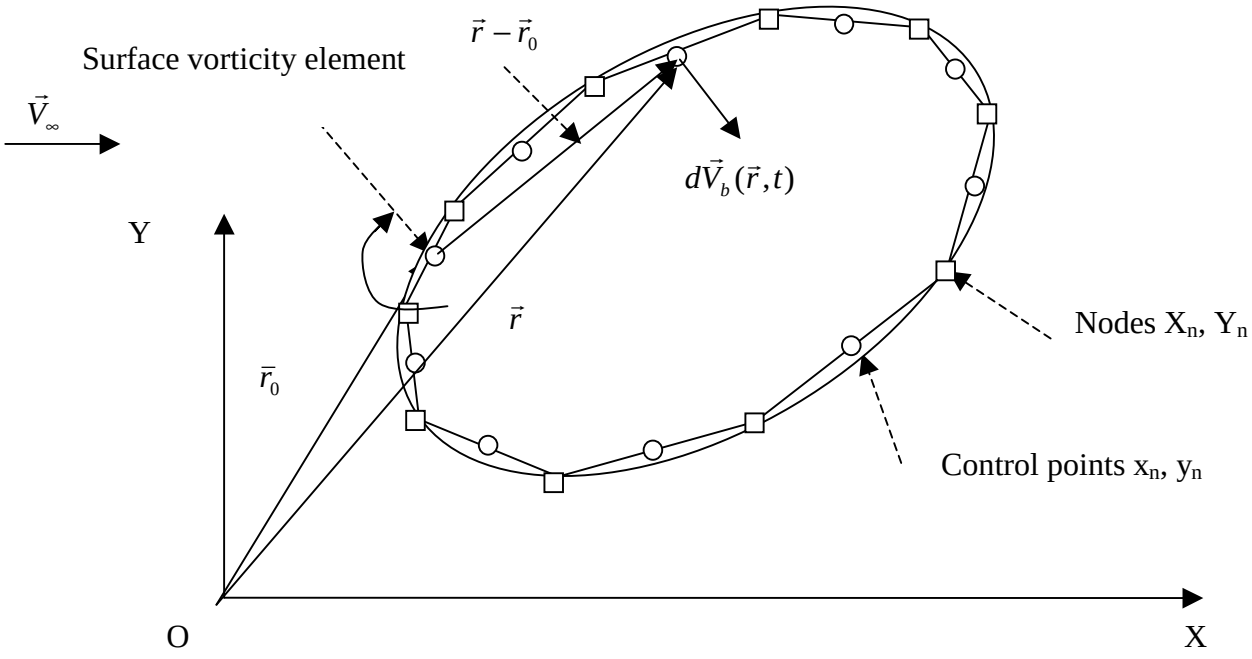

Fig. 3.3 Discrete surface vorticity model for a two-dimensional body

The velocity $d\vec{V}_b(\vec{r},t)$ induced at $\vec{r}$ due to a vorticity element with circulation $\gamma(l(\vec{r}_0),t)ds$ located at $\vec{r}_0$ elsewhere on the body, is obtained from the Biot-Savart law equation (3.3.2.3), which in this case reduces to the velocity induced by a rectilinear vortex, namely

$$d\vec{V}_b(\vec{r},t) = -\frac{1}{2\pi}\vec{e}_z \times \frac{\gamma[l(\vec{r}_0),t](\vec{r}-\vec{r}_0)}{\left|\vec{r}-\vec{r}_0\right|^2} ds(\vec{r}_0) \qquad (3.3.3.1)$$

where $\vec{e}_z$ is a unit vector perpendicular to the (x, y) plane so as to form a right-hand system with the base vectors in the plane of the flow.

By integrating along the contour of the body surface, we obtain the velocity $\vec{V}_b$ induced by the vorticity sheet representing the body surface

$$\vec{V}_b(\vec{r},t) = -\frac{1}{2\pi}\vec{e}_z \times \oint_C \frac{\gamma[l(\vec{r}_0),t](\vec{r}-\vec{r}_0)}{\left|\vec{r}-\vec{r}_0\right|^2} dl(\vec{r}_0) \qquad (3.3.3.2)$$

The vorticity is continuously distributed along the body surface. Consequently, the values of γ in adjoining elements are equal at the common points where the two are connected, the so-called nodes as shown in Fig. 3.4. Along the element, the values of γ within each element are then approximated as a linear function as shown in Fig. 3.4.

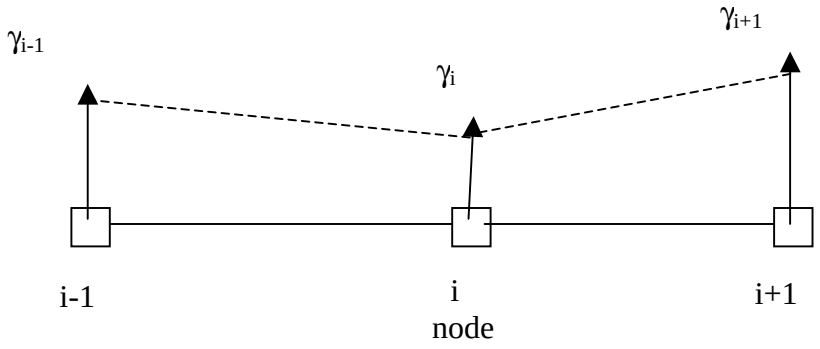

Fig. 3.4 Linearly distributed vorticity

The calculation of the velocity induced by the vorticity on the individual elements is facilitated by introducing a local coordinate system as shown in Fig. 3.5. The origin of the local frame of reference for element i is placed at node i, the local x-axis runs along the element, and the local y-axis points outwards from the body surface into the flowfield.

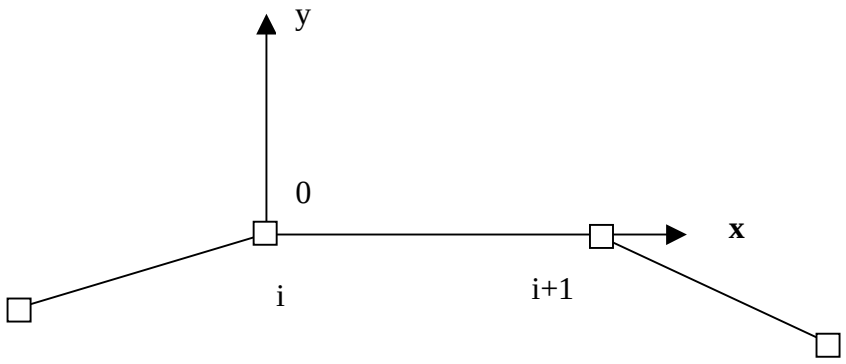

Fig. 3.5. Local coordinate system for vorticity element

The transformations between the local coordinate system and the global coordinate system are then given by

$$\begin{Bmatrix} x \\ y \end{Bmatrix} = \begin{bmatrix} d_1 & d_2 \\ -d_2 & d_1 \end{bmatrix} \begin{Bmatrix} X - X_i \\ Y - Y_i \end{Bmatrix} \qquad (3.3.3.3a)$$

$$\begin{Bmatrix} \vec{e}_x \\ \vec{e}_y \end{Bmatrix} = \begin{bmatrix} d_1 & d_2 \\ -d_2 & d_1 \end{bmatrix} \begin{Bmatrix} \vec{E}_x \\ \vec{E}_y \end{Bmatrix} \qquad (3.3.3.3b)$$

where (x,y) are the coordinates in the local frame with the base vectors $(\vec{e}_x, \vec{e}_y)$, (X,Y) are the coordinates in the global frame with the base vectors $(\vec{E}_x, \vec{E}_y)$, and (X_i, Y_i) are the global coordinates of the node that serves as the origin of the local frame, and

$$\begin{aligned} d_1 &= (X_{i+1} - X_i)/\Delta l_i \\ d_2 &= (Y_{i+1} - Y_i)/\Delta l_i \end{aligned} \qquad (3.3.3.4)$$

where

$$\Delta l_i = \sqrt{(X_{i+1} - X_i)^2 + (Y_{i+1} - Y_i)^2} \qquad (3.3.3.5)$$

is the length of the element i.

The two linear basis functions

$$f_1(\xi) = 1 - \frac{\xi}{\Delta l_i} \qquad (3.3.3.6a)$$

and

$$f_2(\xi) = \frac{\xi}{\Delta l_i} \qquad (3.3.3.6b)$$

are then used to describe γ on each element. This description gives

$$\gamma(\xi,t)_i = G_i(t)\, f_1(\xi) + G_{i+1}(t)\, f_2(\xi) \qquad (3.3.3.7)$$

where $0 \le \xi \le \Delta l_i$, G_i and G_{i+1} are the values of γ at nodes i and i+1, and Δl_i is given by Equation (3.3.3.5).

From Equation (3.3.3.2), it follows that, in the local frame, the components of the velocity induced by the vorticity on a single element are given by

$$\begin{aligned} \vec{V}_{bi}(x,y,t) &= \frac{1}{2\pi}\int_0^{\Delta l_i} \frac{\gamma(\xi,t)_i[y\vec{e}_x - (x-\xi)\vec{e}_y]}{(x-\xi)^2 + y^2}\, d\xi \\ &= G_i[v_{1xi}\vec{e}_x + v_{1yi}\vec{e}_y] + G_{i+1}[v_{2xi}\vec{e}_x + v_{2yi}\vec{e}_y] \end{aligned} \qquad (3.3.3.8)$$

where

$$\begin{aligned} v_{1xi} &= \frac{1}{2\pi\Delta l_i}[(\Delta l_i - x)\Delta\theta - 0.5\, y \ln R] \\ v_{1yi} &= \frac{1}{2\pi\Delta l_i}[y\Delta\theta - \Delta l_i + 0.5(\Delta l_i - x)\ln R \\ v_{2xi} &= \frac{1}{2\pi\Delta l_i}(x\Delta\theta + 0.5\, y \ln R) \\ v_{2yi} &= \frac{1}{2\pi\Delta l_i}(\Delta l_i - y\Delta\theta + 0.5\, x \ln R) \end{aligned} \qquad (3.3.3.9)$$

where

$$\Delta\theta = \tan^{-1}\left(\frac{x}{y}\right) - \tan^{-1}\left(\frac{x-\Delta l_i}{y}\right) \qquad (3.3.3.10)$$

and

$$R = \frac{(x - \Delta l_i)^2 + y^2}{x^2 + y^2} \qquad (3.3.3.11)$$

Applying the inverse transformation of Equation (3.3.3.3) leads to the velocity induced by element i in terms of components in the global frame

$$\vec{V}_{bi}(X,Y,t) = G_i[V_{1Xi}\vec{E}_X + V_{1Yi}\vec{E}_y] + G_{i+1}[V_{2Xi}\vec{E}_X + V_{2Yi}\vec{E}_Y] \qquad (3.3.3.12)$$

where

$$\begin{Bmatrix} V_{kXi} \\ V_{kYi} \end{Bmatrix} = \begin{bmatrix} d_1 & -d_2 \\ d_2 & d_1 \end{bmatrix} \begin{Bmatrix} v_{kxi} \\ v_{kyi} \end{Bmatrix} \qquad (3.3.3.13)$$

for k=1 and 2

No-penetration boundary condition on the surface of the body becomes,

$$\vec{V} \bullet \vec{n} = 0 \qquad (3.3.3.14)$$

where $\vec{V}$ is given by

$$\vec{V} = \vec{V}_b + \vec{V}_\infty \qquad (3.3.3.15)$$

and $\vec{n}$ is a vector normal to the contour of the body.

In applying vorticity modeling as explained above to determine the flow characteristics over a surface-mounted prism, we replace the solid surfaces of the prism by vorticity elements. The details of this substitution are given in Chapter 4. We also model the vorticity generated in the boundary layer and convected into the flow at the separating corners by introducing vortex blobs at the corners. This is also explained in Chapter 4. When comparing the flow modeling as discussed here to the turbulent flow simulations as presented in section 3.2, we note the following:

- By introducing vortex blobs at the corner and following their fate as they convect over a suitable region, we focus on a fluid element as it moves through the flow. Thus, the flow is described using a Lagrangian approach, instead of the Eulerian approach used when solving Navier-Stokes. Unlike grid-based methods, there is no need to define a computational grid or region for the flow.
- Although the inviscid-flow assumption is made, it should be stressed that vorticity is introduced into the flow and, thus some turbulence aspects of the outer flow are obtained. The only problem is that the effect of the vorticity present in the boundary layer on the separation regions is not taken into consideration. However, it should be stressed that the vorticity generated in the boundary layer is allowed to convect from the corners.
- The major difference with a realistic flow is the fact that the solution here is two-dimensional while the real flow is three-dimensional. However, this problem can be solved by having vorticity distribution over the three-dimensional surface of the prism. It must be stated that this extension will require significant work and computer resources.
- The surface vorticity modeling as presented here does not allow for viscous dissipation of the vorticity. This is in contrast to the viscous terms presented in the Navier-Stokes equations which allow for dissipation of turbulence energy.